AMERICAN SOCIETY of
GENE & CELL
THERAPY

Complement-Mediated Activation of the NLRP3 Inflammasome and Its Inhibition by AAV-Mediated Delivery of CD59 in a Model of Uveitis

Binit Kumar,[1] Siobhan M. Cashman,[1] and Rajendra Kumar-Singh[1]

[1]Department of Developmental, Molecular and Chemical Biology, Tufts University School of Medicine, Boston, MA 02111, USA

Uveitis is an inflammatory disorder of the eye responsible for approximately 10%–15% of blindness in the US. In this study, we examined the role of the complement membrane attack complex (MAC) and the NLRP3 inflammasome in the pathogenesis of experimental autoimmune uveitis (EAU) in normal and $C9^{-/-}$ mice that are incapable of assembling the MAC. We discovered that the MAC and the NLRP3 inflammasome and associated production of IL-1β are elevated in EAU mice and that MAC may be involved in regulation of Th1 and Th17 cell differentiation. In contrast, MAC and the NLRP3 inflammasome were not elevated in $C9^{-/-}$ mice. However, EAU-associated pathophysiology including retinal structure and function were not rescued in $C9^{-/-}$ mice. Unexpectedly, AAV-mediated delivery of sCD59, an inhibitor of C9 incorporation into the MAC, successfully attenuated activation of the NLRP3 inflammasome and EAU pathology as well as MAC. Our studies provide an improved understanding of the role of the MAC and the NLRP3 inflammasome in EAU as well as suggest a novel approach for the treatment of uveitis.

INTRODUCTION

Uveitis is a chronic ocular inflammatory disorder of the uveal and retinal layers of the eye responsible for approximately 10%–15% of total blindness in the US.[1] Uveitis is classified as infectious or non-infectious, involving an immune response to an external biological agent or an autoimmune reaction, respectively. The current standard of clinical care requires the use of corticosteroids, immunosuppressive drugs, or monoclonal antibodies, but these approaches have limited success and are associated with significant side effects.[2,3] Thus, there is an unmet clinical need to develop efficacious therapies for autoimmune uveitis (EAU).

Immunization of mice with a peptide derived from retinal interphotoreceptor retinoid-binding protein (IRBP) results in T cell-mediated autoimmune disease analogous to the clinical and histological features observed in human uveitis.[4,5] This experimental model of EAU is thus a commonly used approach for the study of uveitis and for the development of therapies for this disease.

Complement is a critical component of the innate immune system and its role has been described in various inflammatory diseases,

including autoimmune diseases, cancer, ischemia/reperfusion injury, etc.[6] A role for complement has also been previously implicated in EAU,[7–10] although little is known about the mechanisms that connect activation of complement with T cell-mediated pathology in EAU. Activation of complement terminates with the assembly of the membrane attack complex (MAC) on the membrane of cells, resulting in the formation of a pore that at sublytic levels allows for ion exchange across the plasma membrane and the release of cytokines. At higher levels, deposition of MAC can lead to cell lysis. The role of MAC in the pathophysiology of EAU is as yet undetermined. Entry of Ca^{2+} into the cell following deposition of MAC has recently been found to activate the NLRP3 inflammasome in primary lung human epithelial cells.[11]

The NLRP3 inflammasome has been previously implicated in various inflammatory disorders including age-related macular degeneration, cardiomyopathy, arthritis, chronic kidney disease, neurodegenerative diseases etc.[12] Administration of lipopolysaccharide (LPS) in mice leads to MAC associated interleukin (IL)-1β maturation.[13] Although the inflammasome is highly regulated by complement and is necessary during resolution of tissue injury or disease, the unregulated inflammasome can lead to severe inflammation and damage to host tissues.[14] Activation of the NLRP3 inflammasome is controlled by a two-step process that requires an initial priming signal which involves increased expression of the protein NLRP3 and a subsequent activation signal required for formation of the inflammasome protein complex that results in Caspase-1-mediated cleavage of pro-IL-1β into mature IL-1β.[15] Unregulated IL-1β expression can lead to the development of autoimmune and autoinflammatory diseases, including Behçet's disease, Vogt-Koyanagi-Harada disease, rheumatic diseases, autoimmune thyroid disease, insulin-dependent diabetes mellitus, gout, familial Mediterranean fever, and cryopyrin-associated periodic syndromes.[16–18] Further, it has recently been found that IL-1β is actively secreted in the retina by myeloid cells, indicating a potential
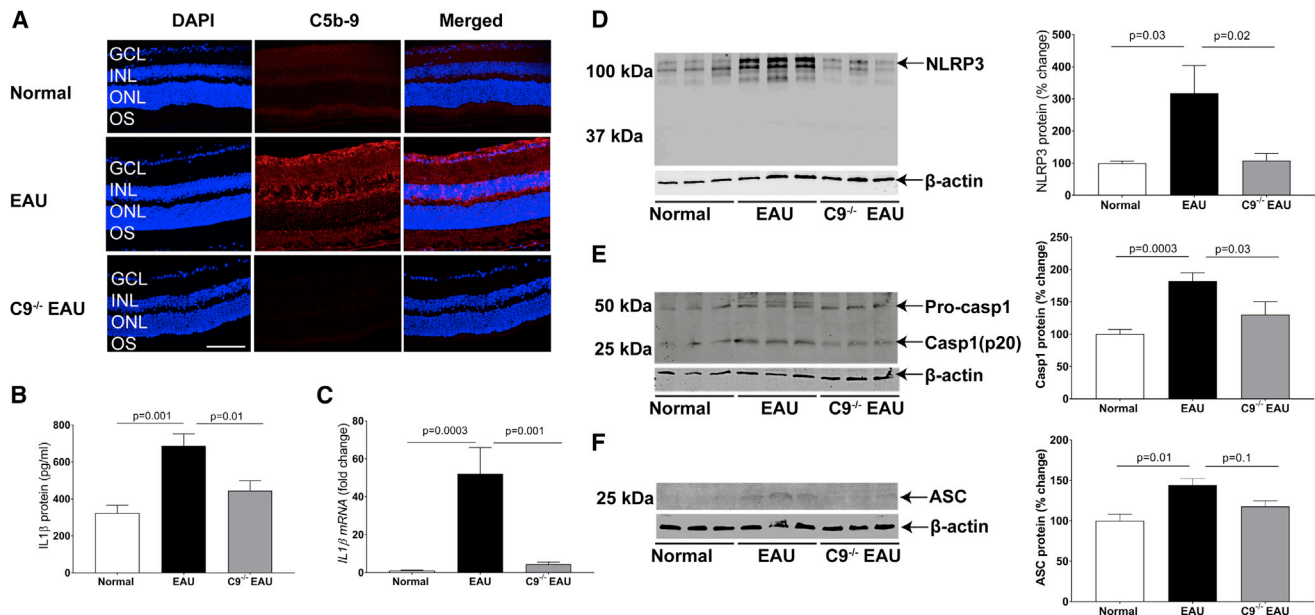
Figure 1. MAC-Mediated NLRP3 Inflammasome Activation Increases IL-1β Production in EAU

(A) Representative retinal cryostat sections stained with C5b-9 antibody, indicating elevated MAC formation in EAU retina relative to normal retina. As anticipated, $C9^{-/-}$ EAU mouse retina remained negative for MAC. For quantification of MAC fluorescence intensity, refer to Figure S1. (B and C) Production of IL-1β, as measured by ELISA (B) and real-time PCR (C) in EAU retinas, was significantly higher than normal control retinas. However, moderate increases in IL-1β protein and mRNA levels in $C9^{-/-}$ EAU retinas were found relative to normal control retinas. (D and E) Western blot indicated an increase in NLRP3 (D) and Caspase-1 (p20) (E) protein expression in EAU retinas relative to normal control retinas. However, a small increase was recorded in $C9^{-/-}$ EAU retinas relative to normal control retinas. (F) Western blot indicating an increase in ASC protein expression in EAU retinas relative to normal control retinas. However, the levels of ASC in $C9^{-/-}$ EAU mice retinas were only marginally higher relative to normal control retinas. The western blot and real-time PCR values were normalized to β-actin. Values are represented as mean ± SEM. GCL, ganglion cell layer; INL, inner nuclear layer; ONL, outer nuclear layer; OS, outer segments; scale bar, 100 μm.

pathogenic role of IL-1R signaling in EAU.[19] However, detailed mechanisms of how IL-1β is regulated in EAU remains elusive.

In order to further understand the potential mechanism by which MAC may be involved in the pathogenesis of EAU and to elucidate the importance of NLRP3 activation and production of IL-1β in the development of EAU, we test the hypothesis that MAC is deposited in EAU retina, and that MAC may be necessary for the activation of the NLRP3 inflammasome and subsequent release of IL-1β.

MAC is comprised of one molecule each of C5b, C6, C7, C8, and up to 12 C9 molecules. Since $C9^{-/-}$ mice cannot assemble a functioning MAC, we hypothesized that such mice may be partially protected from EAU. In order to test the above hypothesis, we induced EAU in C57BL/6J mice and compared the induced pathology to that of EAU in $C9^{-/-}$ mice. In order to evaluate the therapeutic potential of inhibiting C9 in EAU, we subsequently utilized a gene therapy approach using an adeno-associated virus (AAV) expressing a soluble CD59 (AAVCAGsCD59)—a protein that prevents the incorporation of C9 into the preformed C5b-8 complex. We monitored the development of EAU in AAVCAGsCD59-injected mice by fundus imaging, spectral domain optimal coherence tomography (SD-OCT), retinal histopathology and immunohistochemistry. Retinal function was quantified by the electroretinogram (ERG) and NLRP3 inflamma-

some activation was measured by western blots, ELISA, and real-time PCR. Our results implicate for the first time a direct role for MAC as an activator of the NLRP3 inflammasome and IL-1β production in the development of EAU. We have also demonstrated for the first time that AAV-mediated expression of soluble CD59 is a potential gene therapy for the treatment of EAU.

RESULTS
MAC Deposition in EAU
The final step in the activation of complement results in the deposition of the MAC on the surface of cells. Recruitment of multiple C9 molecules into the pre-formed C5b-8 complex is the final and necessary step in the assembly of the MAC (C5b-9). Mice deficient in C9 are thus theoretically unable to form functional MAC complexes. In order to determine whether MAC is formed on the surface of retinal cells in EAU, we examined frozen retinal sections at 24 days post-induction of EAU in C57BL/6J mice by staining with antibody against C5b-9. We found that there was 70% greater MAC on the retina of EAU mice relative to normal controls. Furthermore, we found no significant MAC on the surface of $C9^{-/-}$ EAU retina (Figures 1A and S1). We conclude that complement is activated in EAU and that the reaction reaches completion to form MAC on retinal tissues. We also conclude that $C9^{-/-}$ EAU mice are unable to form MAC on the retina.

Activation of the Inflammasome in EAU

Deposition of MAC on the surface of cells leads to the formation of a pore and thus an increase in intracellular calcium. We examined whether deposition of MAC triggered activation of the NLRP3 inflammasome and subsequent secretion of IL-1β. We found that EAU in C57BL/6J mice led to a 112% increase in IL-1β protein and a corresponding 45-fold increase in IL-1β mRNA. In contrast, $C9^{-/-}$ EAU mice achieved only a 37% increase in IL-1β protein and a corresponding 3.8-fold increase in IL-1β mRNA (Figures 1B and 1C). Western blot analyses indicated that there was a 200% increase in NLRP3 protein in EAU mice, whereas $C9^{-/-}$ EAU mice had only an 8% increase in NLRP3 protein (Figure 1D). Another important component of the inflammasome complex is Caspase-1, which normally occurs in an inactive zymogen form, activated by NLRP3 complex by proteolysis into active p10 and p20 subunits to make the final multimeric inflammasome complex. Western blot analyses indicated an 80% increase in the activation of Caspase-1 (p20) in EAU retinas; however, $C9^{-/-}$ EAU mouse retinas had only 25% activation of Caspase-1(p20) (Figure 1E). We also measured ASC protein expression, an inflammasome adaptor protein, in EAU retinas by western blot. Western blot analyses indicated that there was a 44% increase in ASC protein in EAU mice, whereas $C9^{-/-}$ EAU mice had only an 18% increase in ASC protein (Figure 1F).

We conclude that IL1-β, NLRP3, Caspase-1, and ASC are all elevated in EAU and that $C9^{-/-}$ EAU mice are partially protected from such increase, suggesting that deposition of MAC may be an important player in the activation of the inflammasome in EAU.

Potential Role of MAC-Mediated NLRP3 Inflammasome Activation in T Cell Differentiation in EAU

CD4+ infiltrating T cells enter the retina either differentiated or undifferentiated into Th1, interferon (IFN)-γ-producing cells, and Th17, IL-17 producing cells. In order to investigate the potential role of the MAC in T cell differentiation, we measured the levels of IFN-γ and IL-17 in EAU and $C9^{-/-}$ EAU mice retinas, respectively.

Using ELISA, we found that in EAU retinas there was a 102% increase in IFN-γ protein relative to normal C57BL/6J retinas. In contrast, there was a 14% decrease in IFN-γ protein relative to normal C57BL/6J retinas in $C9^{-/-}$ EAU retinas. Real-time PCR indicated a more than 200-fold and 14-fold increases in IFN-γ mRNA in EAU and $C9^{-/-}$ EAU retinas, respectively, relative to normal C57BL/6J retinas (Figures S2A and S2B). Similarly, we found that there was 99% greater IL-17 protein in EAU retinas relative to normal C57BL/6J retinas, whereas there was only a 44% increase in IL-17 protein in $C9^{-/-}$ EAU retinas. In contrast, we did not find any statistical difference between the levels of IL-17 mRNA between EAU and $C9^{-/-}$ EAU retinas. Also, IL-17 mRNA levels remained below the detection limit in C57BL/6J retinas (Figures S2C and S2D). These observations suggest that MAC may play a role in T cell differentiation in EAU.

Next, we examined the levels of Th1 and Th17 CD4+ cells in draining lymph nodes (DLNs) at 24 days post-EAU in normal C57BL/6J, EAU, and $C9^{-/-}$ EAU mice. We found a significantly greater number of IL-17 and IFN-γ-positive CD4+ cells in the DLNs of EAU mice relative to normal C57BL/6J mice (Figures S3A–S3C). However, there was no statistically significant difference in the levels of IFN-γ- and IL-17-positive CD4+ cells in DLNs between EAU and $C9^{-/-}$ EAU mice (Figures S3A–S3C). These results suggest that whereas MAC may play a significant role in T cell differentiation in the retina in EAU, it may not play a significant role in DLNs.

Role of the MAC on Retinal Function in EAU

We measured retinal function in EAU and $C9^{-/-}$ EAU mice using ERG. Relative to normal C57BL/6J mice, EAU mice had dark-adapted a-wave amplitudes that were reduced by 33%, 50%, and 41% at flash intensities of −20 dB, −10 dB, and 0 dB, respectively. $C9^{-/-}$ EAU mice had a-wave amplitudes that were also reduced but by a lesser extent, specifically 9%, 40%, and 27% at flash intensities of −20 dB, −10 dB, and 0 dB, respectively, relative to normal controls (Figures 2A and 2B).

Dark-adapted b-wave amplitudes in EAU mice were reduced by 47%, 52%, and 49% at flash intensities of −20 dB, −10 dB, and 0 dB, respectively. $C9^{-/-}$ EAU mice had dark-adapted b-wave amplitudes that were also reduced but by a lesser extent, specifically 32%, 33%, and 17% at flash intensities of −20 dB, −10 dB, and 0 dB, respectively, relative to normal C57BL/6J controls. Although we found differences in both the a-wave and b-wave dark-adapted ERGs between EAU and $C9^{-/-}$ EAU mice, only the b-wave at 0 dB was statistically ($p < 0.05$) significant (Figures 2A and 2B).

Relative to normal mice, EAU mice had light adapted b-wave amplitudes that were reduced by 44% and 37% at flash intensities of 0 dB and 1 dB, respectively. $C9^{-/-}$ EAU mice had b-wave amplitudes that were reduced by 5% and 15% at flash intensities of 0 dB and 1 dB, respectively. Although we found differences in light-adapted b-wave amplitudes between EAU and $C9^{-/-}$ EAU mice, only the 0 dB was statistically ($p < 0.05$) significant (Figures 2A and 2B).

No Significant Preservation of Retinal Structure in $C9^{-/-}$ EAU

In anticipation that $C9^{-/-}$ mice may be protected from EAU, we quantified retinal structure and pathological severity of disease in EAU and $C9^{-/-}$ EAU mice using fundus imaging, OCT, and histology at 24 days post-induction of EAU. Based on clinical scoring criteria developed by others,[20] fundus imaging revealed that EAU mice had severe inflammation as expected—specifically, an overall clinical score 16-fold greater than the control group, including a 38-fold increase in vascular inflammation, 8-fold increase in infiltration of immune cells, 13-fold increase in damage to the optic disc, and 34-fold increase in structural damage relative to normal C57BL/6J mice. Unexpectedly, $C9^{-/-}$ mice undergoing uveitis had pathological outcomes statistically equivalent to EAU mice (Figure 3).

Twenty-four days post-immunization, EAU mice exhibited a severe inflammatory cellular infiltration into the vitreous and choroid along with retinal vasculitis, retinal edema and a moderate to severe retinal
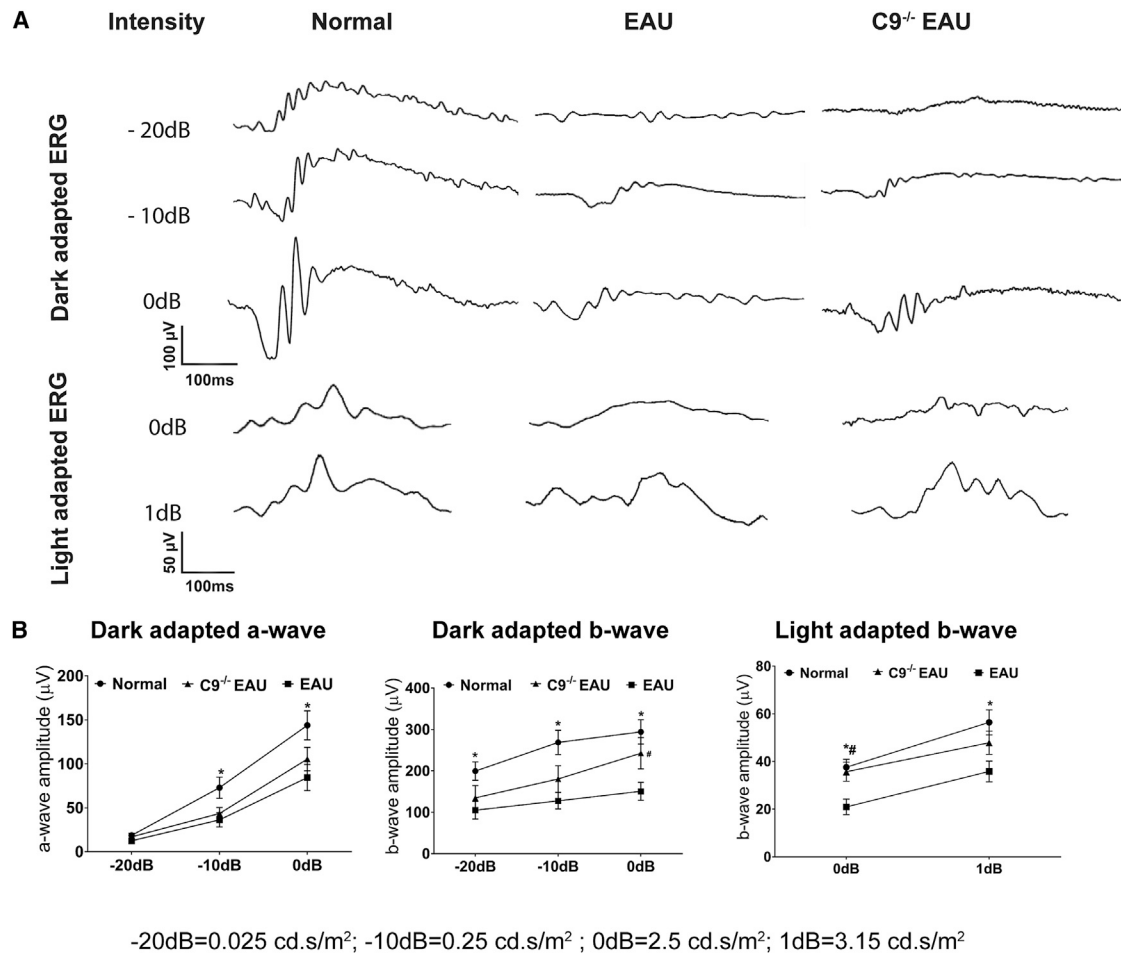
Figure 2. Effects of MAC Formation on Retinal Function in EAU

EAU results in extensive damage to photoreceptors, which impairs retinal function. Dark-adapted (scotopic) and light-adapted (photopic) responses were analyzed in normal, EAU, and $C9^{-/-}$ EAU mouse retinas. For dark-adapted ERGs, −20 dB (0.025 cd.s/m^2), −10 dB (0.25 cd.s/m^2), and 0 dB (2.5 cd.s/m^2) flash light intensities were used. For light-adapted ERGs, 0 dB (2.5 cd.s/m^2) and 1 dB (3.15 cd.s/m^2) flash light intensities were used. (A) Representative ERG responses in normal, EAU, and $C9^{-/-}$ EAU groups. (B) Dark- and light-adapted a- and b-wave ERG amplitudes with respect to intensities are shown. Values are represented as mean ± SEM.*$p < 0.05$, #$p < 0.05$ versus EAU.

folding and infiltrates relative to normal C57BL/6J control mice as shown by OCT imaging and histopathology (Figures 4A and 4B). A detailed histological analysis was performed in paraffin-embedded sections from normal control, EAU and $C9^{-/-}$ EAU mice retinas and scored based on criteria developed by others.[4] Based on criteria developed by others,[4] the photoreceptor damage score was calculated as a combined score of photoreceptor loss, retinal folds, and retinal detachment. Similarly, the infiltration score was comprised of a combination of granuloma, hemorrhage, Dalen-Fuchs (DF) nodule, and infiltrates. Vasculitis score represents perivascular inflammation and CD4 cell infiltration around vasculature, formation of thrombi, and extent of vasculature affected in the retina. We found that EAU mice had approximately 27-fold more infiltrates (Figure 4C), increased vasculitis (Figure 4D), and 78-fold greater photoreceptor damage (Figure 4E) than normal C57BL/6J control mice. Although the histological score in $C9^{-/-}$ EAU mice had 28% less infiltration,

35% lower photoreceptor damage, and 31% reduced vasculitis than that found in EAU mice, the differences were not statistically significant (Figures 4C–4E).

Soluble CD59-Mediated Inhibition of MAC Deposition in EAU

Above, we discovered that mice unable to form MAC due to a genetic defect in C9 are unable to activate the inflammasome and that they are protected from some select features of uveitis. However, the retina of $C9^{-/-}$ EAU mice was not protected from the histological pathology associated with EAU. Nonetheless, we wished to examine whether inhibition of MAC by interfering with the incorporation of C9 into C5b-8 using a gene therapy approach instead of a genetic approach may yield contrasting outcomes.

CD59 is a glycosyl-phosphatidylinositol (GPI)-anchored protein found on the membrane of most nucleated cells. The major function of CD59
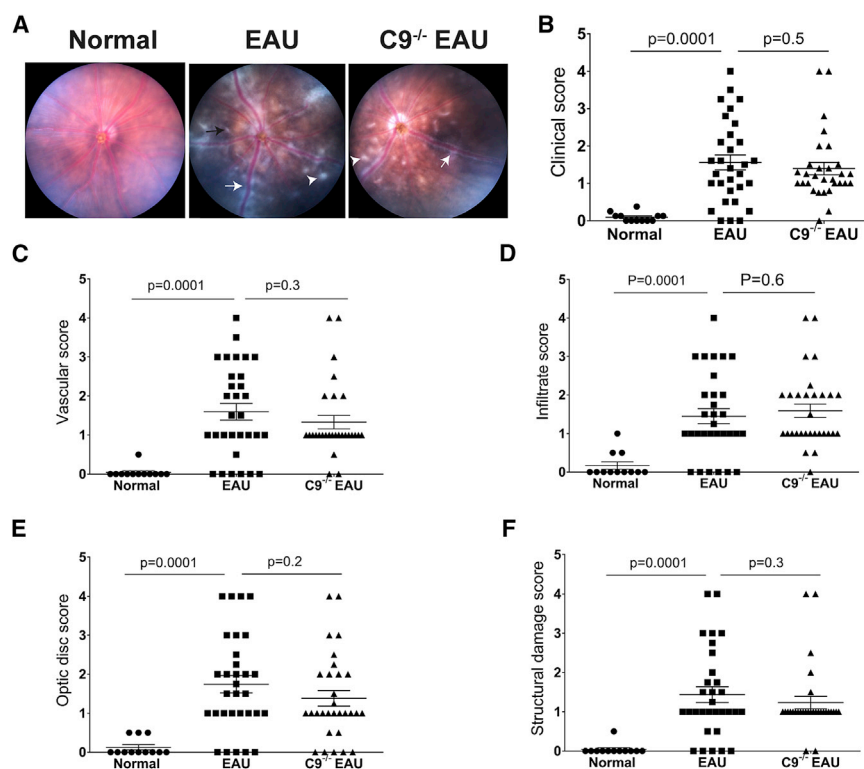
Funduscopic EAU severity was analyzed after 24 days of EAU among normal, EAU, and *C9$^{-/-}$* EAU mice. Focal lesions, linear lesions, vasculitis, retinal hemorrhages, infiltrates, and retinal detachment were examined. According to the severity of these findings, the EAU clinical scores were graded on a scale of 0–4. (A) Fundus images from EAU and *C9$^{-/-}$* EAU group showing retinal inflammatory infiltrates (white arrowhead), vasculitis (white arrow), and retinal folds (black arrow). (B–F) Overall clinical score (B) and individual scores for vasculature (C), cellular infiltrations (D), optic disc (E), and structural damage (F). Values are represented as mean ± SEM.

undergoing EAU. In order to address whether similar outcomes could be achieved using a gene therapy approach with sCD59, we measured NLRP3/Caspase-1-mediated secretion of IL-1β in EAU mice that were pre-injected with either AAVCAGsCD59 or AAVC AGGFP as described above. AAVCAGsCD59-injected EAU mice had 40% and 70% less IL-1β protein and mRNA, respectively, relative to AAVCAGGFP-injected EAU mice as measured by ELISA and real-time PCR, respectively (Figures 5B and 5C). Similarly, NLRP3 protein and Caspase-1 p20 levels were reduced by 60% in AAVCAGsCD59-injected EAU mice relative to AAVC AGGFP-injected EAU mice (Figures 5D and 5E). However, we did not find any statistically significant difference between the expression of ASC in AAVCAGsCD59-injected EAU mice relative to AAVCA GGFP-injected EAU mice (Figure 5F). In conclusion, our results suggest that sCD59 attenuates NLRP3 mediated IL-1β production by inhibiting MAC deposition in uveitis.

is to prevent the recruitment of C9 into the pre-formed C5b-8 complex. Previously, we have described a recombinant AAV vector expressing a truncated CD59 (AAVCAGsCD59) that has its GPI anchor signal deleted, enabling it to be secreted and diffuse throughout the retina.[21]

Mice were injected intravitreally with AAVCAGsCD59, and 1 week later (to allow for optimal levels of transgene expression), mice were challenged with EAU as described above. As negative controls, we similarly injected mice intravitreally with AAVCAGGFP—a virus expressing GFP that were similarly challenged with EAU. At 24 days post-induction of EAU, we examined frozen retinal sections from both sets of mice by staining with C5b-9 antibody. Intravitreal injection of AAVCAGGFP in mice that were subsequently challenged with EAU led to transgene expression in the ganglion cell layer, inner plexiform layer, and inner nuclear layer (Figure S4). In mice with phenotypically more severe EAU, transgene expression could also be observed in the retinal pigment epithelium (RPE) and photoreceptors (Figure S4).

Our results indicate that AAVCAGsCD59-injected EAU mice had approximately 45% less deposition of MAC relative to AAVCA GGFP-injected EAU mice (Figures 5A and S5). We conclude that intravitreally injected AAVCAGsCD59 can inhibit the formation of MAC in the retina of EAU mice.

Soluble CD59-Mediated Inhibition of the Inflammasome in EAU

Above, we found that *C9$^{-/-}$* EAU mice had significantly reduced activation of the inflammasome relative to normal C57BL/6J mice
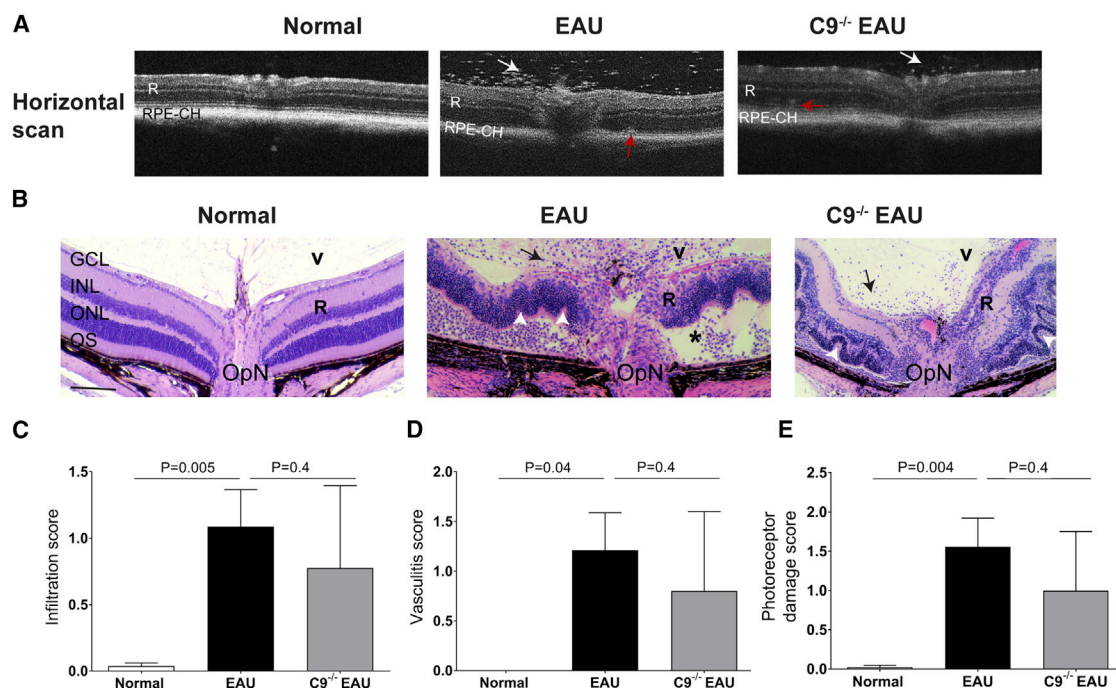
The Impact of Soluble CD59 on T Cell Differentiation in EAU

In order to investigate the potential affects on T cell differentiation in sCD59-expressing eyes undergoing EAU, we measured the levels of IFN-γ and IL-17 protein and mRNA in AAVCAGsCD59-injected EAU mice and AAVCAGGFP-injected EAU mice. The levels of IFN-γ and IL-17 protein were significantly inhibited by more than 25% and 35% in AAVCAGsCD59-injected EAU retinas relative to AAVCAGGFP-injected EAU retinas (Figures S6A and S6C). Further, the levels of IFN-γ and IL-17 mRNA from freshly isolated AAV CAGsCD59-injected EAU retinas revealed a 47% and 10% inhibition, respectively, relative to AAVCAGGFP-injected EAU retinas. However, differences in mRNA expression were not deemed statistically significant (Figures S6B and S6D).

Soluble CD59-Mediated Preservation of Retinal Function in EAU

In order to determine whether sCD59 could preserve retinal function in EAU, we performed ERGs in AAVCAGsCD59-injected or AAVC AGGFP-injected mice undergoing uveitis. Relative to AAVCAG GFP-injected mice, AAVCAGsCD59-injected EAU mice had

Figure 4. Retinal Imaging and Histology in EAU and *C9*$^{-/-}$ EAU Mice

(A) Horizontal OCT scans showing retinal foldings in the retina (red arrow) and vitreous cellular infiltrates (white arrow) in EAU and *C9*$^{-/-}$ EAU group. (B) Retinal sections (5 μm) were generated from paraffin-embedded eyes on day 24 post-EAU induction and stained with H&E. Infiltration of inflammatory immune cells in the vitreous (V) are shown by black arrows; black asterisk represents retinal (R) detachment; retinal folds are shown by white arrowheads. (C–E) Severity of EAU pathology is represented by individually scoring infiltration (C), vasculitis (D), and photoreceptor damage (E), as described in the Materials and Methods and Results. Values are represented as mean ± SEM. RPE-CH, RPE and choroid; R, retina; V, vitreous; GCL, ganglion cell layer; INL, inner nuclear layer; ONL, outer nuclear layer; OS, outer segments; OpN, optic nerve. Scale bar, 100 μm.

dark-adapted larger a-wave amplitudes by 45%, 49%, and 51% at flash intensities of −20 dB, −10 dB, and 0 dB, respectively. Similarly, the dark-adapted b-wave amplitudes in AAVCAGsCD59-injected mice were larger by 55%, 48%, and 40% at −20 dB, −10 dB, and 0 dB flash intensities, respectively, relative to AAVCAGGFP-injected EAU control eyes (Figure 6). Further, the light adapted b-wave amplitude at 0 dB and 1 dB flash intensity in AAVCAGsCD59-injected EAU eyes were preserved by 12% and 39% relative to AAVCAGGFP-injected control EAU eyes (Figure 6). These data support a significant potentially therapeutic role for recombinant sCD59 in preserving retinal function in the inner and outer retina in uveitis.

Soluble CD59-Mediated Preservation of Retinal Structure and Pathology in EAU

In order to determine whether sCD59 could preserve retinal structure and reduce pathology associated with uveitis, we performed fundus imaging of AAVCAGsCD59-injected or AAVCAGGFP-injected EAU mice. Again, based on scoring criteria developed by others,[20] we determined that the overall clinical score in AAVCAGsCD59-injected EAU mice was 22% less than in AAVCAGGFP-injected EAU mice. The overall clinical score comprised of the appearance of 24% fewer inflammatory infiltrates, 27% less structural damage, 22% reduced vasculitis and cuffing of vessels and, 13% less damage

to the optic disc in AAVCAGsCD59-injected EAU mice relative to AAVCAGGFP-injected EAU mice (Figures 7A–7F). There was no significant difference found between PBS vehicle control and AAVCAGGFP-injected EAU retinas. Whereas the vascular, infiltration, and structural damage scores were all statistically significantly different (p < 0.05), the optic disc score did not reach the same levels of statistical significance (p = 0.2). Overall, we conclude that expression of sCD59 reduced retinal inflammation and infiltration of immune cells in uveitis.

The progression and severity of EAU was greater in AAVCAGGFP-injected EAU mice relative to AAVCAGsCD59-injected EAU mice as recorded in OCT scans (Figure 8A). We performed detailed histological analysis of paraffin sections taken from the retina of PBS-injected EAU mice, AAVCAGsCD59-injected EAU, mice or AAVCAGGFP-injected EAU mice. Based on criteria developed by others,[4] we found that AAVCAGsCD59-injected EAU mice had approximately 76% fewer infiltrates, 69% less photoreceptor damage, and 78% less vasculitis than AAVCAGGFP-injected EAU mice (Figures 8B–8E). Whereas photoreceptor damage and infiltration were statistically significant (p = 0.03 and p = 0.01, respectively), the vasculitis score was not found to be statistically significant (p = 0.2).
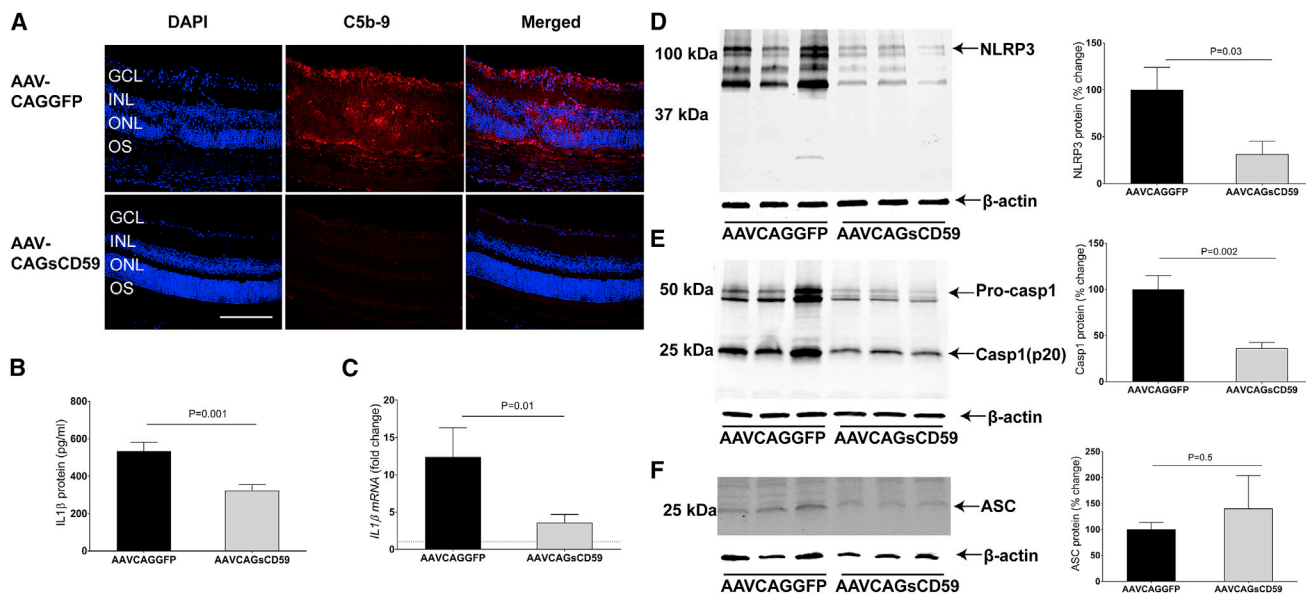
Figure 5. Soluble CD59 Inhibits NLRP3 Inflammasome Activation and IL-1β Production in EAU

(A) Retinal cryostat sections from AAVCAGsCD59- and AAVCAGGFP-injected eyes were stained with C5b-9 antibody. For quantification of MAC fluorescence intensity, refer to Figure S5. (B and C) Production of IL-1β, as measured by ELISA (B) and real-time PCR (C) in AAVCAGsCD59 mouse retinas was significantly lower than AAVCAGGFP retinas (40% and 70%, respectively). (D and E) Western blot showing greater than 60% decrease in both NLRP3 (D) and Caspase-1 (p20) (E) protein expression in AAV CAGsCD59-injected retinas relative to AAVCAGGFP-injected retinas. (F) Western blot showing insignificant change in ASC protein expression in AAVCAGsCD59 retinas relative to AAVCAGGFP retinas. The western blot and real-time PCR values are normalized to β-actin. Values are represented as mean ± SEM. GCL, ganglion cell layer; INL, inner nuclear layer; ONL, outer nuclear layer; OS, outer segments. Scale bar, 100 μm.

DISCUSSION

In this study, we investigated for the first time the direct role of MAC in the activation of the NLRP3 inflammasome in EAU. We report three main findings from our work. First, our studies demonstrate that MAC is deposited in the EAU retina and this results in activation of the NLRP3 inflammasome and increased production of IL-1β. Second, we report that $C9^{-/-}$ EAU mice fail to form MAC on their retina and concomitantly have attenuated activation of the NLRP3 inflammasome, strongly suggesting a link between deposition of MAC and activation of the NLRP3 inflammasome in EAU. Third, we report that even though $C9^{-/-}$ mice fail to rescue the EAU pathological phenotype, AAV-mediated delivery of sCD59, an inhibitor of C9 incorporation into C5b-8, unexpectedly attenuates many aspects of the EAU pathological phenotype, including activation of the NLRP3 inflammasome.

The complement system is a major component of innate immunity and consists of a diverse group of plasma and membrane-bound proteins. These proteins play a central role in protection against pathogens and in the regulation of immune and inflammatory processes. The activation of complement against pathogens for host defense is necessary, but over-activated complement may inflict damage to host tissues.[6,22] Therefore, it is necessary to maintain a balance between complement activation and complement inhibition through complement regulatory proteins. Over-activated and unregulated complement terminates in the formation of MAC that has previously been shown to be involved in a variety of ocular disorders, including EAU.[7–9,23,24] However, the direct role of MAC deposition in the pathogenesis of EAU remained to be investigated. Here, we demonstrate that MAC is deposited in EAU, and this leads to increased production of IL-1β. However, $C9^{-/-}$ EAU mice lack the ability to form MAC and consequently have reduced levels of IL-1β. This led us to investigate the link between MAC and IL-1β production in EAU.

Although MAC deposition on cell membranes eventually results in cell death by lysis, sub-lytic MAC on cell membranes has been implicated in for example regulation of cell cycle and proliferation, apoptosis, production of cytokines, and initiation of downstream signaling cascades.[6] The NLRP3 inflammasome complex is a group of cytoplasmic proteins consisting of a primary regulatory subunit NLRP3, an adaptor subunit ASC, and the effector subunit Caspase-1, which converts pro-IL-1β into active IL-1β.[14,15] Recent studies in LPS-primed models have reported that sub-lytic MAC-induced pore formation, leading to an accumulation of intracellular Ca^{2+} that subsequently led to activation of the NLRP3 inflammasome.[11,13] The NLRP3 inflammasome has been previously implicated in several ocular diseases.[25,26] We thus contemplated whether attenuation of the activation of NLRP3 inflammasome may be a novel therapeutic approach for the treatment of uveitis. Our studies indicated for the first time the direct role of MAC and NLRP3 inflammasome activation in the EAU mouse model. We demonstrated that MAC directly activated and increased protein expression of NLRP3, Caspase-1, and
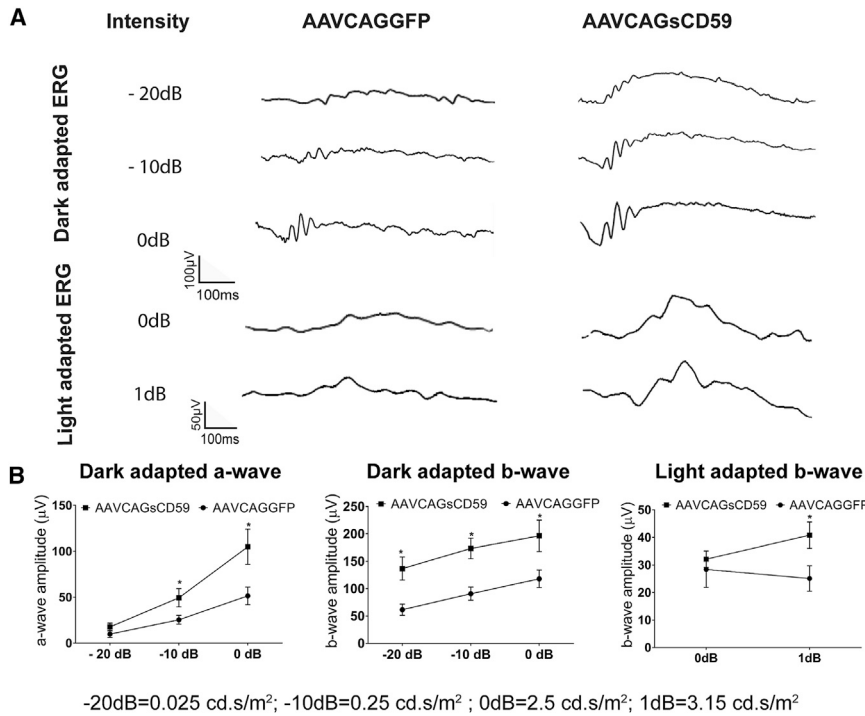
A

ASC subunits. These activated subunits form the NLRP3 inflammasome complex that produces active IL-1β. As anticipated, $C9^{-/-}$ EAU mice did not activate the NLRP3 inflammasome and IL-1β remained close to basal levels, confirming activation of the NLRP3 inflammasome as a MAC-dependent pathway.

Autoreactive effector CD4$^+$ T cells are associated with pathogenesis in EAU. Both Th1 and Th17 lineages are specifically responsible in the development of EAU and have been reported in uveitis patients.[27,28] Also, IL-1β signaling promotes differentiation of CD4$^+$ T cells into Th17 cells.[29] More recent studies have found that blocking the IL-1 signaling pathway is promising for the treatment of EAU in mice.[19] The IL-1R antagonist *anakinra*, soluble decoy IL-1R *rilonacept*, and IL-1b-neutralizing antibody *canakinumab* have been approved for the treatment of uveitis.[2] However, multiple side effects and short duration of action makes them limited in use. In agreement with prior studies, we found increased production of IL-1β in EAU retinas; however, lower levels of IL-1β were discovered in $C9^{-/-}$ EAU mouse retinas. Further, we found increased differentiation of Th1 and Th17 cells in the EAU retinas; however, decreased Th1 and Th17 cells in the $C9^{-/-}$ EAU retinas as interpreted from the respective IL-17 and IFN-γ protein and mRNA levels, respectively. Furthermore, we found increased levels of Th1- and Th17-positive CD4 cells in DLNs from EAU mice, but levels remained unchanged in DLNs from $C9^{-/-}$ EAU mice. Therefore, we suggest that MAC-induced IL-1β production and differentiation of Th1 and Th17 cells in EAU retina is a local effect.

Many complement regulatory proteins are secreted or found on the surface of cells to keep complement-mediated damage to host tissues in check. These proteins include factor H, decay-accelerating factor (CD55), membrane cofactor protein (CD46), and protectin (CD59). The decreased activity or deficiency of these complement regulatory proteins can lead to immunopathologies including EAU and experimental autoimmune anterior uveitis.[6,7,22,30] EAU is a chronic and multifactorial disease associated with systemic disease. Various studies have found that inhibition of complement activation may help in ameliorating EAU pathology in mice.[7–9] Therefore, we envisaged the use of a long-acting gene therapy approach utilizing AAV to deliver sCD59 to EAU mice. Here, we show for the first time that AAVCAGsCD59 inhibits MAC deposition in EAU retina. AAVCAGsCD59 also successfully inhibited the activation of the NLRP3 inflammasome and attenuated IL-1β production.

Furthermore, a single intravitreal injection of AAVCAGsCD59 also successfully inhibited some of the phenotypic pathologies in EAU mice. In these same mice, the clinical signs associated with EAU were significantly improved, including reduced inflammation, fewer immune cell infiltrates, and reduced vasculitis. We also found that AAVCAGsCD59 injection led to an improvement in loss of retinal function associated with EAU in both dark- and light-adapted ERGs. Whereas $C9^{-/-}$ mice displayed statistically significant inhibition of activation of the NLRP3 inflammasome and a reduced upregulation of IL-1β, we noticed only a trend of improved histology score and improved retinal function in $C9^{-/-}$ EAU mice—the differences did not reach a significant level of statistical significance except for a few data points in ERG.

Unexpectedly, our studies do suggest that AAVCAGsCD59 possibly attenuates inflammation by a means other than blocking incorporation of C9 into the C5b-8 complex. GPI-anchored CD59 has been previously reported to bind to CD2 and transduce activation signals within T cells.[31] CD59 cross-linking induces T cell receptor zeta/ZAP-70 signaling cascade and IL-2 synthesis. IL-2 has been found
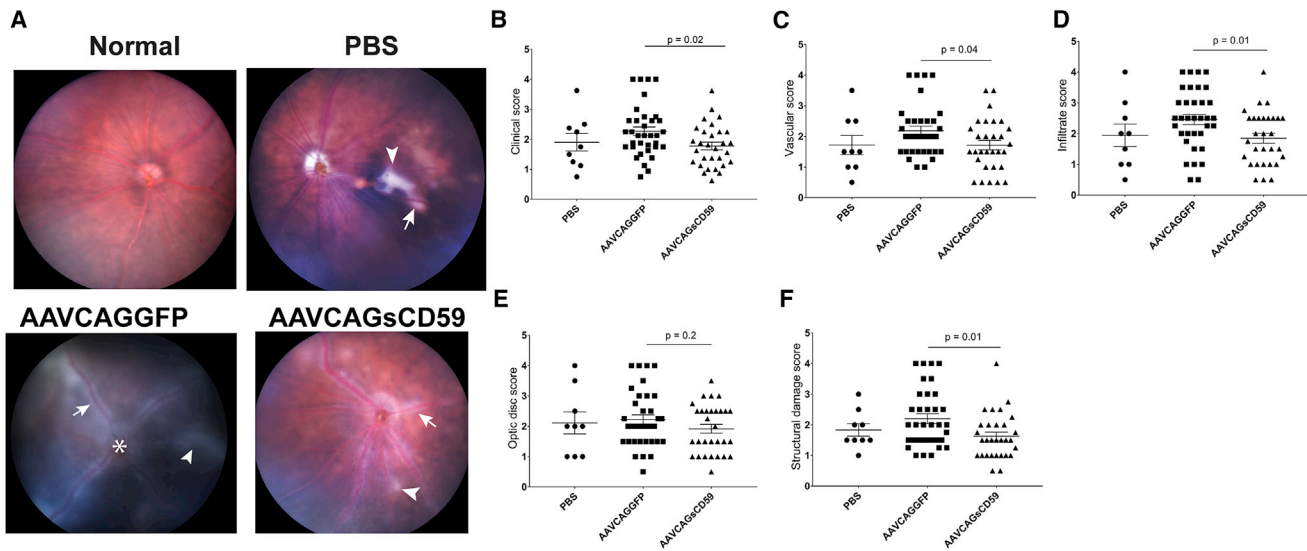
Figure 7. Soluble CD59 Attenuates the Severity of Clinical Score in EAU

The funduscopic EAU severity was analyzed in PBS-, AAVCAGGGFP-, and AAVCAGsCD59-injected EAU mice. The EAU clinical scores were graded on a scale of 0–4. (A) Representative fundus images from PBS-, AAVCAGsCD59-, and AAVCAGGGFP-injected group showing retinal inflammatory infiltrates (white arrowhead), vasculitis (white arrow), and papilledema (white asterisk). (B–F) AAVCAGsCD59 group showing statistically significant improved individual scores for overall clinical score (B), vasculature (C), cellular infiltration (D), and structural damage (F), compared with AAVCAGGGFP group. However, optic disc scores (E) remained statistically insignificant between AAV CAGsCD59- and AAVCAGGGFP-injected group. The differences between PBS and AAVCAGGGFP-injected eyes remained statistically insignificant. Values are represented as mean ± SEM.

to be successful in modulating the immune system in diseases including type 1 diabetes and vasculitis,[32] supporting the hypothesis that sCD59 may attenuate inflammation in a MAC-independent manner. The EAU model we utilized for studying uveitis has inconsistencies related to mild-to-moderate EAU development. These minor changes may also contribute to our observations. Most recently, an alternative peptide has been developed that has shown an improvement in the consistency of pathology in EAU and severity of disease[33]—use of such peptides may reduce the level of variation observed in our own studies in EAU.

Uveitis is a chronic inflammatory disease, and many patients face episodes of relapse and some of them are refractory to available therapies. Overall, conventional therapies remain limited in managing severe and advanced stages of uveitis in patients with systemic autoimmune disease (Bechet's disease, Vogt-Koyanagi disease, etc.) due to significant side effects and short-term efficacy. The treatment for managing uveitis has not advanced significantly during the previous few decades.[2] Considering these issues, it is practical to develop a long-acting therapy such as the continuous inhibition of MAC-dependent activation of the inflammasome in uveitis patients. Therefore, single intravitreal injection of AAVsCD59 has significant potential and advantages relative to the short-term effect of present therapies. Recently, many laboratories including our own have shown that AAV-dependent gene therapies are successful in treating ocular diseases in animal models.[34,35] Moreover, AAV-mediated gene therapies have successfully advanced into human clinical trials for age-related macular degeneration.[36]

Despite the above promising results, our study has some limitations. First, we injected intravitreal AAVCAGsCD59 1 week before inducing uveitis in mice. The reason for this approach was to allow for the time necessary for ramping up of transgene expression and secretion of sCD59. Therefore, our study is prophylactic in nature. Second, in our present study, the clinical ocular scores were 20% higher in AAVCAGGGFP-injected eyes compared with PBS vehicle control, suggesting a possible contribution of AAV itself to some ocular inflammation, although it was statistically insignificant. Moreover, IFN-γ and IL-17 protein levels in EAU and AAVCAGGFP EAU were essentially equivalent, strongly suggesting that AAV does not contribute toward inflammation. Although we did not notice any significant adverse effects in these short-term proof-of-concept studies, long-term studies will need to be performed to evaluate the safety of AAVCAGsCD59 for the treatment of uveitis.

In summary, in this study, we demonstrated that MAC is an important regulator of NLRP3 inflammasome activation and production of IL-1β in EAU. Also, MAC plays an important role in differentiation of Th1 and Th17 cells via increasing IL-1β production. AAV-mediated expression of sCD59 was efficient in successfully inhibiting MAC deposition and subsequent inhibition of NLRP3 inflammasome activation. A single intravitreal injection of AAVCAGsCD59 was efficacious in inhibiting the development of EAU in mice. Therefore, we propose that AAV CAGsCD59 deserves further study as a potential treatment for uveitis.
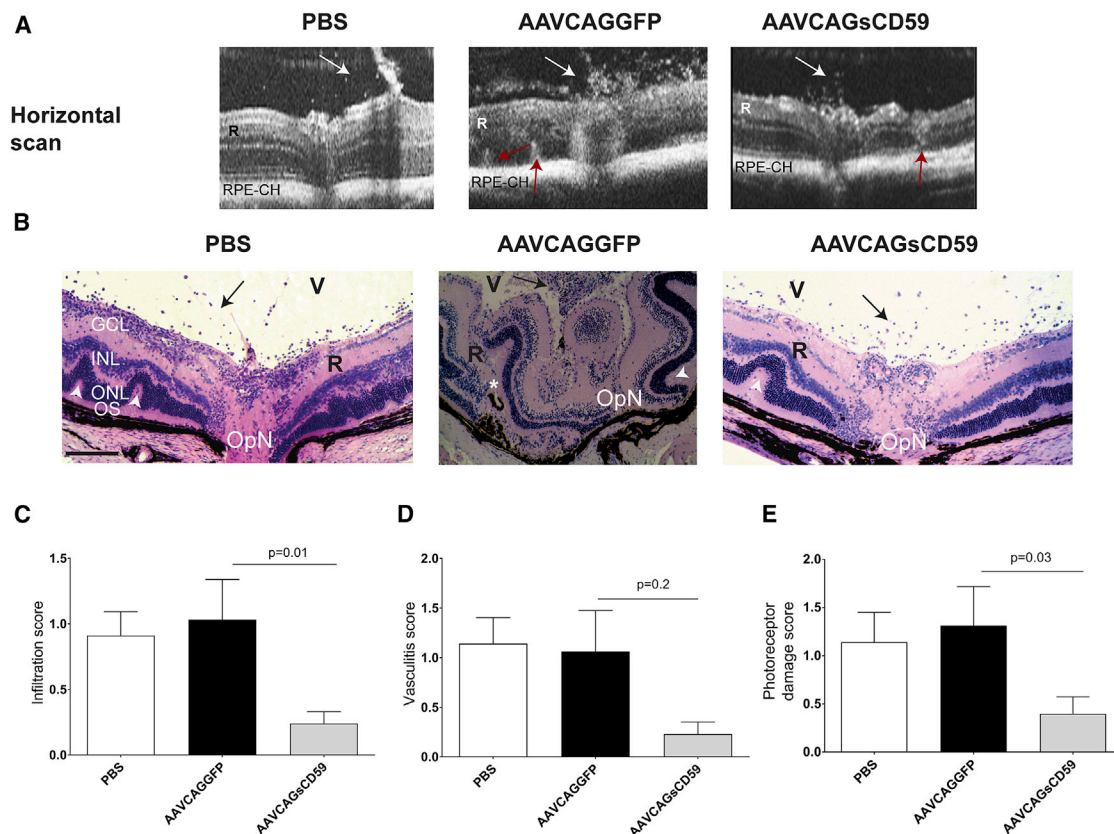
Figure 8. Effect of sCD59 on OCT Changes and Retinal Histology Score in EAU

(A) Horizontal OCT scans showing retinal foldings in the retina (red arrow) and vitreous cellular infiltrates (white arrow) in AAVCAGGFP-injected or AAVCAGsCD59-injected or PBS-injected EAU mice. (B) Retinal sections (5 μm) were generated from paraffin-embedded eyes on day 24 post-EAU induction and stained with H&E. Infiltration of inflammatory immune cells in the vitreous (V) are shown by black arrows; white asterisk represents retinal (R) detachment; retinal folds are shown by white arrowheads. (C–E) Severity of EAU pathology is represented by individual infiltration (C), vasculitis (D), and photoreceptor damage (E) as described in the Materials and Methods. Values are represented as mean ± SEM. RPE-CH, RPE and choroid; R, retina; V, vitreous; GCL, ganglion cell layer; INL, inner nuclear layer; ONL, outer nuclear layer; OS, outer segments; OpN, optic nerve. Scale bar, 100 μm.

MATERIALS AND METHODS

Mice

C57BL/6J and $C9^{-/-}$ mice on the C57BL/6J background were purchased from The Jackson Laboratory (Bar Harbor, ME) and maintained in the animal facilities at Tufts University School of Medicine, Boston. All animal study protocols conformed to the Association for Research in Vision and Ophthalmology resolution on the use of Animals in Vision Research and the recommendations of the National Institutes of Health Guide for the Care and Use of Laboratory Animals.

AAV Constructs and Intravitreal Injections

We have previously described construction of an AAV serotype 2 vector expressing a truncated form of human CD59 or *protectin* (AAVCAGsCD59) that has its GPI anchoring signal deleted.[21] The soluble CD59 (sCD59) is expressed from a chicken β-actin promoter. As a negative control, we utilized a similar vector expressing GFP (AAVCAGGFP). Six-week-old C57BL/6J mice were injected with

3.5×10^9 genome copies/μL of AAVCAGsCD59 or AAVCAGGFP or PBS (1 μL) and 1 week later challenged with EAU as described below.

Induction of EAU by Active Immunization

Six-week-old C57BL/6J and $C9^{-/-}$ mice on the same genetic background were immunized with 200 μg of human IRBP peptide 1–20 (GPTHLFQPSLVLDMAKVLLD; Biomatik Corporation, Cambridge, ON, Canada) emulsified in 200 μL of 1:1 v/v complete Freund's adjuvant (CFA) containing *Mycobacterium tuberculosis* strain H37RA (2.5 mg/mL). The mice simultaneously received 1.5 μg *Bordetella pertussis* toxin diluted in 100 μL PBS via intraperitoneal injection.[37]

Immunohistochemistry

Cryostat retinal sections (10 μm) were rehydrated in PBS for 15 min, blocked with 6% normal goat serum in PBS for 1 hr, and incubated overnight in a moist chamber with the primary antibody against rabbit anti-human C5b-9 (Complement Technology, Tyler, TX;

dilution: 1:800, diluted in PBS containing 2% normal goat serum). Subsequently, sections were washed and incubated with anti-rabbit secondary antibody conjugated to Cy3 (Molecular Probes, Eugene, OR) to localize C5b-9 in retinal sections. Slides were mounted in anti-fade medium containing DAPI (Vectashield-DAPI; Vector Laboratories, Burlingame, CA) to counterstain the nuclei, and images were captured with a Leica confocal microscope. The intensity of C5b-9 staining over the entire section was quantified using ImageJ software (NIH; Bethesda, MD).

Western Blot Analysis

Murine retinas were harvested and homogenized in ice-cold RIPA buffer containing 50 mM Tris-HCl (pH 7.4), 250 mM NaCl, and 1% Nonidet P-40, with a protease inhibitor cocktail. Each protein sample (35 μg) was separated by SDS-PAGE (Any kD Mini-PROTEAN precast gel, Bio-Rad, CA) for NLRP3, Caspase-1, ASC, and CD59 and then transferred onto nitrocellulose membranes. After blocking with buffer (LI-COR Biosciences, Lincoln, NE, USA), mixed with 0.1% Tween 20, immunoblots were incubated overnight at 4°C with mouse anti-NLRP3 monoclonal, mouse anti-Caspase-1 monoclonal, rabbit anti-ASC polyclonal (Adipogen Corporation, San Diego, CA; dilution: 1:500), and rabbit anti-CD59 polyclonal (Abcam, Cambridge, MA; dilution: 1:500) as the primary antibodies. Following incubation with the appropriate secondary antibody, the immunoreactive bands were visualized using LI-COR-Odyssey infrared scanner (LI-COR Biosciences). The blots were re-probed with β-actin as a loading control.

Enzyme-Linked Immunosorbent Assay

The cytokines were quantified by sandwich ELISA for mouse IL-1β, IFN-γ, and IL-17 (PeproTech, Rocky Hills, NJ), per the manufacturer's instructions using 20 μg retinal protein supernatant. Supernatants were added in duplicate, and the cytokine being measured was revealed with a monoclonal antibody conjugated to horseradish peroxidase. The concentration of cytokines is reported in pg/mL.

Gene Expression

Total RNA was isolated from mouse retina using the RNeasy mini kit (QIAGEN, Valencia, CA) according to the manufacturer's protocol. RNA was quantified by 260 nm absorbance in a "Nanodrop," and 1 μg RNA was used for cDNA synthesis using the High-Capacity cDNA reverse transcription kit (Applied Biosystems, Foster City, CA).

Real-time PCR was performed using predesigned TaqMan primers for β-actin (Mm02619580_g1), IL-1β (Mm00434228_m1), IL-17 (Mm00439619_m1), and IFN-γ (Mm01168134_m1). Denaturation was performed at 95°C for 10 min, followed by 40 cycles at 95°C for 15 s, and annealing and extension were performed at 60°C for 60 s. The final PCR products were electrophoresed on a 2% agarose gel to confirm PCR specificity. The Ct values obtained from the real-time PCR were normalized to the Ct value from β-actin in the same sample using the ddCt method, and fold-change in gene expression was reported. Gene expression for IL-17 was quantified semiquantitatively.

Flow Cytometry

DLN cells were isolated from mice and single-cell suspensions generated by passing the cells through a 40-μm nylon mesh. DLN cells were stimulated with 50 ng/mL phorbol 12-myristate 13-acetate (PMA) and 500 ng/mL ionomycin (Sigma-Aldrich, St Louis, MO) for 4 hr in the presence of GolgiStop (BD Biosciences, San Jose, CA) before intracellular cytokine staining. Cells were first stained for the surface markers CD4 and then fixed with Cytofix/Cytoperm Buffer (BD Biosciences, San Jose, CA) for cytokine staining. Cells were stained with appropriately diluted fluorophore-labeled antibodies against intracellular targets (IFN-γ, IL-17; eBiosciences, San Diego, CA) along with respective isotype controls in Perm/Wash buffer (BD Biosciences, San Jose, CA). Flow cytometry was performed on a FACS Calibur (BD Biosciences), and data were analyzed with FlowJo software (Tree Star, Ashland, OR). Gates were set based on appropriate isotype controls. Where indicated, the percentage of positive cells represents the percentage in the gated population relative to normal controls.

ERG

Scotopic and photopic ERG analysis was used to measure the loss of rod and cone function. Three weeks after EAU induction, ERGs were recorded using a UTAS system with BigShot ganzfeld (LKC Technologies; Gaithersburg, MD). Following dark adaptation overnight, mice were anesthetized with ketamine (100 mg/kg)/xylazine (10 mg/kg) intraperitoneal injection under dark conditions. The pupils were dilated with 1% tropicamide and 2.5% phenylephrine hydrochloride. ERG-active contact lens gold electrodes were placed gently on the center of cornea with a drop of lubricant (GenTeal, Alcon, Fort Worth, TX) to maintain corneal hydration and better electrical conductivity. Reference and ground electrodes were inserted subcutaneously to the back of the neck and near the tail base, respectively. Scotopic ERGs were elicited with 10 ms flashes of white light at 0 dB (2.5 cd.s/m^2), −10 dB (0.25 cd.s/m^2), and −20 dB (0.025 cd.s/m^2). Simultaneously, photopic ERGs were examined after a 2-min white-light bleach. The photopic responses were elicited with flashes of white light at 0 dB and 1 dB (3.15 cd.s/m^2) intensity. Ten responses were averaged at every flash intensity. The amplitude of the a-wave was measured from the baseline to the negative peak of a-wave, and the b-wave was measured from the negative peak of the a-wave to the peak of the b-wave.

Spectral Domain OCT and Fundus Imaging

Mice were anesthetized with a ketamine and xylazine cocktail and pupils dilated with a drop of 1% tropicamide and 2.5% phenylephrine, and the cornea was kept moistened by topical application of eye lubricant (GenTeal, Alcon, Fort Worth, TX). OCT images were acquired using a Bioptigen Spectral Domain Ophthalmic Imaging System (Bioptigen Envisu R2300, Morisville, NC). Averaged single B scan and volume scans were obtained with images centered on the optic nerve head as described previously.[38]

After 24 days of EAU, fundus imaging was performed and images captured using a Micron III Retinal Imaging Microscope and

StreamPix software (Phoenix Research Labs, Pleasanton, CA). Specifically, eyes were examined for infiltrates, cuffing around the blood vessels, white linear lesions, retinal dystrophy, subretinal hemorrhages, and retinal detachment. An individual score was evaluated by two independent observers in a blinded fashion on a scale of 0–4 for individual parameters: retinal infiltrates, optic disc changes, vascularity, and structural damage. Clinical scores were calculated by averaging the score for each of these four criteria.[20]

Histopathology

Eyes for histologic examination from all groups were harvested at 24 days post-immunization and fixed in 10% buffered formalin. After fixation for 2 days, specimens were dehydrated through graded alcohol steps and embedded in paraffin blocks. Six vertical sections (5 μm) were cut at six different planes including the optic nerve region and stained with H&E. The detailed severity of EAU was assessed on a scale of 0–4 for photoreceptor damage, and infiltration and vasculitis was as described previously by others.[4] Based on these criteria, the photoreceptor damage score was calculated as a combined score of photoreceptor loss, retinal folds, and retinal detachment. Similarly, the infiltration score was comprised of a combination of granuloma, hemorrhage, DF Nodule, and infiltrates. Vasculitis score represents perivascular inflammation and immune cell infiltration around vasculature, formation of thrombi, and extent of vasculature affected in the retina.

Statistical Analysis

Experimental results are shown as mean ± SEM. Mann-Whitney test was used for a clinical score, histology score, and FACS analysis. Statistical differences between two groups were analyzed using an unpaired t test. For comparison between more than two groups, one-way ANOVA was performed. A p value of less than or equal to 0.05 was considered statistically significant.

SUPPLEMENTAL INFORMATION

Supplemental Information includes six figures and can be found with this article online at https://doi.org/10.1016/j.ymthe.2018.03.012.

AUTHOR CONTRIBUTIONS

Study Design, R.K.-S., B.K., S.M.C.; Experiment Design and Implementation, B.K., R.K.-S.; Data Analysis, B.K.; Manuscript Preparation, B.K., R.K.-S.; Manuscript Review and Editing, B.K. and R.K.-S.; Funding Acquisition, R.K.-S.

ACKNOWLEDGMENTS

REFERENCES

1. Durrani, O.M., Meads, C.A., and Murray, P.I. (2004). Uveitis: a potentially blinding disease. Ophthalmologica 218, 223–236.

2. Knickelbein, J.E., Armbrust, K.R., Kim, M., Sen, H.N., and Nussenblatt, R.B. (2017). Pharmacologic treatment of noninfectious uveitis. Handb. Exp. Pharmacol. 242, 231–268.

3. Prete, M., Dammacco, R., Fatone, M.C., and Racanelli, V. (2016). Autoimmune uveitis: clinical, pathogenetic, and therapeutic features. Clin. Exp. Med. 16, 125–136.

4. Caspi, R.R., Roberge, F.G., Chan, C.C., Wiggert, B., Chader, G.J., Rozenszajn, L.A., Lando, Z., and Nussenblatt, R.B. (1988). A new model of autoimmune disease. Experimental autoimmune uveoretinitis induced in mice with two different retinal antigens. J. Immunol. 140, 1490–1495.

5. Chan, C.C., Caspi, R.R., Ni, M., Leake, W.C., Wiggert, B., Chader, G.J., and Nussenblatt, R.B. (1990). Pathology of experimental autoimmune uveoretinitis in mice. J. Autoimmun. 3, 247–255.

6. Morgan, B.P., and Harris, C.L. (2015). Complement, a target for therapy in inflammatory and degenerative diseases. Nat. Rev. Drug Discov. 14, 857–877.

7. An, F., Li, Q., Tu, Z., Bu, H., Chan, C.C., Caspi, R.R., and Lin, F. (2009). Role of DAF in protecting against T-cell autoreactivity that leads to experimental autoimmune uveitis. Invest. Ophthalmol. Vis. Sci. 50, 3778–3782.

8. Copland, D.A., Hussain, K., Baalasubramanian, S., Hughes, T.R., Morgan, B.P., Xu, H., Dick, A.D., and Nicholson, L.B. (2010). Systemic and local anti-C5 therapy reduces the disease severity in experimental autoimmune uveoretinitis. Clin. Exp. Immunol. 159, 303–314.

9. Read, R.W., Szalai, A.J., Vogt, S.D., McGwin, G., and Barnum, S.R. (2006). Genetic deficiency of C3 as well as CNS-targeted expression of the complement inhibitor sCrry ameliorates experimental autoimmune uveoretinitis. Exp. Eye Res. 82, 389–394.

10. Zhang, L., Bell, B.A., Yu, M., Chan, C.C., Peachey, N.S., Fung, J., Zhang, X., Caspi, R.R., and Lin, F. (2016). Complement anaphylatoxin receptors C3aR and C5aR are required in the pathogenesis of experimental autoimmune uveitis. J. Leukoc. Biol. 99, 447–454.

11. Triantafilou, K., Hughes, T.R., Triantafilou, M., and Morgan, B.P. (2013). The complement membrane attack complex triggers intracellular Ca2+ fluxes leading to NLRP3 inflammasome activation. J. Cell Sci. 126, 2903–2913.

12. Amin, J., Boche, D., and Rakic, S. (2017). What do we know about the inflammasome in humans? Brain Pathol. 27, 192–204.

13. Laudisi, F., Spreafico, R., Evrard, M., Hughes, T.R., Mandriani, B., Kandasamy, M., Morgan, B.P., Sivasankar, B., and Mortellaro, A. (2013). Cutting edge: the NLRP3 inflammasome links complement-mediated inflammation and IL-1β release. J. Immunol. 191, 1006–1010.

14. Latz, E., Xiao, T.S., and Stutz, A. (2013). Activation and regulation of the inflammasomes. Nat. Rev. Immunol. 13, 397–411.

15. Broz, P., and Dixit, V.M. (2016). Inflammasomes: mechanism of assembly, regulation and signalling. Nat. Rev. Immunol. 16, 407–420.

16. Dinarello, C.A., and van der Meer, J.W. (2013). Treating inflammation by blocking interleukin-1 in humans. Semin. Immunol. 25, 469–484.

17. Gabay, C., Lamacchia, C., and Palmer, G. (2010). IL-1 pathways in inflammation and human diseases. Nat. Rev. Rheumatol. 6, 232–241.

18. Jesus, A.A., and Goldbach-Mansky, R. (2014). IL-1 blockade in autoinflammatory syndromes. Annu. Rev. Med. 65, 223–244.

19. Wan, C.K., He, C., Sun, L., Egwuagu, C.E., and Leonard, W.J. (2016). Cutting edge: IL-1 receptor signaling is critical for the development of autoimmune uveitis. J. Immunol. 196, 543–546.

20. Xu, H., Koch, P., Chen, M., Lau, A., Reid, D.M., and Forrester, J.V. (2008). A clinical grading system for retinal inflammation in the chronic model of experimental autoimmune uveoretinitis using digital fundus images. Exp. Eye Res. 87, 319–326.

21. Cashman, S.M., Ramo, K., and Kumar-Singh, R. (2011). A non membrane-targeted human soluble CD59 attenuates choroidal neovascularization in a model of age related macular degeneration. PLoS ONE 6, e19078.

22. Carroll, M.V., and Sim, R.B. (2011). Complement in health and disease. Adv. Drug Deliv. Rev. *63*, 965–975.

23. Gehrs, K.M., Jackson, J.R., Brown, E.N., Allikmets, R., and Hageman, G.S. (2010). Complement, age-related macular degeneration and a vision of the future. Arch. Ophthalmol. *128*, 349–358.

24. Yanai, R., Thanos, A., and Connor, K.M. (2012). Complement involvement in neovascular ocular diseases. Adv. Exp. Med. Biol. *946*, 161–183.

25. Devi, T.S., Lee, I., Hüttemann, M., Kumar, A., Nantwi, K.D., and Singh, L.P. (2012). TXNIP links innate host defense mechanisms to oxidative stress and inflammation in retinal Muller glia under chronic hyperglycemia: implications for diabetic retinopathy. Exp. Diabetes Res. *2012*, 438238.

26. Tseng, W.A., Thein, T., Kinnunen, K., Lashkari, K., Gregory, M.S., D'Amore, P.A., and Ksander, B.R. (2013). NLRP3 inflammasome activation in retinal pigment epithelial cells by lysosomal destabilization: implications for age-related macular degeneration. Invest. Ophthalmol. Vis. Sci. *54*, 110–120.

27. Amadi-Obi, A., Yu, C.R., Liu, X., Mahdi, R.M., Clarke, G.L., Nussenblatt, R.B., Gery, I., Lee, Y.S., and Egwuagu, C.E. (2007). TH17 cells contribute to uveitis and scleritis and are expanded by IL-2 and inhibited by IL-27/STAT1. Nat. Med. *13*, 711–718.

28. Caspi, R.R., Silver, P.B., Chan, C.C., Sun, B., Agarwal, R.K., Wells, J., Oddo, S., Fujino, Y., Najafian, F., and Wilder, R.L. (1996). Genetic susceptibility to experimental autoimmune uveoretinitis in the rat is associated with an elevated Th1 response. J. Immunol. *157*, 2668–2675.

29. Chung, Y., Chang, S.H., Martinez, G.J., Yang, X.O., Nurieva, R., Kang, H.S., Ma, L., Watowich, S.S., Jetten, A.M., Tian, Q., and Dong, C. (2009). Critical regulation of early Th17 cell differentiation by interleukin-1 signaling. Immunity *30*, 576–587.

30. Jha, P., Sohn, J.H., Xu, Q., Wang, Y., Kaplan, H.J., Bora, P.S., and Bora, N.S. (2006). Suppression of complement regulatory proteins (CRPs) exacerbates experimental autoimmune anterior uveitis (EAAU). J. Immunol. *176*, 7221–7231.

31. Deckert, M., Ticchioni, M., Mari, B., Mary, D., and Bernard, A. (1995). The glycosyl-phosphatidylinositol-anchored CD59 protein stimulates both T cell receptor zeta/ZAP-70-dependent and -independent signaling pathways in T cells. Eur. J. Immunol. *25*, 1815–1822.

32. Hartemann, A., Bensimon, G., Payan, C.A., Jacqueminet, S., Bourron, O., Nicolas, N., Fonfrede, M., Rosenzwajg, M., Bernard, C., and Klatzmann, D. (2013). Low-dose interleukin 2 in patients with type 1 diabetes: a phase 1/2 randomised, double-blind, placebo-controlled trial. Lancet Diabetes Endocrinol. *1*, 295–305.

33. Mattapallil, M.J., Silver, P.B., Cortes, L.M., St Leger, A.J., Jittayasothorn, Y., Kielczewski, J.L., Moon, J.J., Chan, C.C., and Caspi, R.R. (2015). Characterization of a new epitope of IRBP that induces moderate to severe uveoretinitis in mice with H-2b haplotype. Invest. Ophthalmol. Vis. Sci. *56*, 5439–5449.

34. Adhi, M., Cashman, S.M., and Kumar-Singh, R. (2013). Adeno-associated virus mediated delivery of a non-membrane targeted human soluble CD59 attenuates some aspects of diabetic retinopathy in mice. PLoS ONE *8*, e79661.

35. Ildefonso, C.J., Jaime, H., Rahman, M.M., Li, Q., Boye, S.E., Hauswirth, W.W., Lucas, A.R., McFadden, G., and Lewin, A.S. (2015). Gene delivery of a viral anti-inflammatory protein to combat ocular inflammation. Hum. Gene Ther. *26*, 59–68.

36. Mingozzi, F., and High, K.A. (2011). Therapeutic in vivo gene transfer for genetic disease using AAV: progress and challenges. Nat. Rev. Genet. *12*, 341–355.

37. Agarwal, R.K., Silver, P.B., and Caspi, R.R. (2012). Rodent models of experimental autoimmune uveitis. Methods Mol. Biol. *900*, 443–469.

38. Chen, J., Qian, H., Horai, R., Chan, C.C., and Caspi, R.R. (2013). Use of optical coherence tomography and electroretinography to evaluate retinal pathology in a mouse model of autoimmune uveitis. PLoS ONE *8*, e63904.